Available online at website: https://journal.bcrec.id/index.php/bcrec

Bulletin of Chemical Reaction Engineering & Catalysis, 19 (4) 2024, 573-584

Research Article

Enhanced Removal Efficiency of Malachite Green Dye Using Gambier Leaf Extract-Modified NiFe LDH Composites: A Study of Cationic Dye Adsorption

Jefri Jefri[1], Najma Annuria Fithri[3], Aldes Lesbani[1,2*]

[1]Master Program of Materials Science, Graduate School, Universitas Sriwijaya, Palembang 30139, Indonesia
[2]Research Center of Inorganic Materials and Coordination Complexes, Universitas Sriwijaya, Palembang 30139, Indonesia
[3]Department of Pharmacy, Faculty of Mathematics and Natural Sciences, Universitas Sriwijaya, Ogan Ilir 30862, Indonesia

Received: 24th September 2024; Revised: 31th October 2024; Accepted: 1st November 2024
Available online: 3th November 2024; Published regularly: December 2024

Abstract

A NiFe layered double hydroxide (LDH) composite with *Uncaria gambir* (UG) leaf extract was successfully synthesized. The composite (NiFe-UG LDH) and the base material (NiFe LDH) were identified using X-ray Diffraction (XRD), Fourier Transform Infra Red (FTIR), and Brunauer-Emmett-Teller (BET) Surface Area techniques. The XRD and FTIR results revealed the incorporation of gambier leaf extract into the NiFe LDH structure, as indicated by the combined diffraction patterns and spectral features. The BET analysis indicated a decrease in the surface area of NiFe-UG LDH compared to that of NiFe LDH, suggesting that active compounds from the gambier leaf extract effectively coated the LDH surface and blocked its pores. During malachite green (MG) adsorption, NiFe-UG demonstrated faster adsorption kinetics and a higher adsorption efficiency, reaching 96.420% compared to 92.085% for NiFe LDH. While both materials followed pseudo-first-order kinetics, their isotherm behaviors differed: NiFe-UG adhered to the Langmuir model, indicating monolayer adsorption, whereas NiFe LDH followed the Freundlich model, signifying multilayer adsorption. Further analysis suggested that adsorption in NiFe LDH was primarily governed by physisorption, while in NiFe-UG, a combined physisorption-chemisorption mechanism occurred. These results underscore the enhanced adsorption capacity of the composite material, attributed to the introduction of additional functional groups from the gambier leaf extract.

Copyright © 2024 by Authors, Published by BCREC Publishing Group. This is an open access article under the CC BY-SA License (https://creativecommons.org/licenses/by-sa/4.0).

Keywords: NiFe LDH; *Uncaria gambir*; Malachite Green; Physisorption-Chemisorption; Composite

How to Cite: Jefri, J., Fithri, N. A., Lesbani, A. (2024). Enhanced Removal Efficiency of Malachite Green Dye Using Gambier Leaf Extract-Modified NiFe LDH Composites: A Study of Cationic Dye Adsorption. *Bulletin of Chemical Reaction Engineering & Catalysis*, 19 (4), 573-584 (doi: 10.9767/bcrec.20215)

Permalink/DOI: https://doi.org/10.9767/bcrec.20215

1. Introduction

Pollution of the aquatic environment has become an increasing concern. Various types of waste such as dye waste have been found in water bodies [1]. Malachite green ($C_{23}H_{25}ClN_2$) is one of dyes that is often used by industry as a dye for clothing, distilleries, paper, and food [2–4]. In addition, malachite green (MG) is also often used as a neutralizer of bacteria and fungi in the aquaculture industry because of its effectiveness and cheapness [5]. However, the persistent presence of MG in water bodies can cause serious health problems, so methods to deal with it are being addressed [6]. Adsorption is a commonly used method because it is easy to implement and relatively inexpensive [7]. Some materials that have been used in previous studies such as biochar [8], bentonite [9], zeolite [10], and layered double hydroxide (LDH) [11].

* Corresponding Author.
Email: aldeslesbani@pps.unsri.ac.id (A. Lesbani)

LDH is clay-like materials that often function as adsorbents [12–14]. LDH comprises of divalent (M^{2+}) and trivalent (M^{3+}) metal ions, arranged in a layered structure [15,16]. The advantages of LDH include their extensive surface area, high capacity for anion exchange, and their ability to adsorb a wide range of pollutants, such as heavy metals and dyes [17]. LDH is also flexible to be modified with various other materials to improve its adsorption performance, making it a highly potential material for environmental applications [18]. However, LDH has some disadvantages, such as the tendency to peel off or decompose during adsorption, which can reduce its effectiveness [19]. In addition, regeneration of these materials is often not optimal without structural modifications. To solve these disadvantages, LDH is usually composited with other substances, like an organic materials.

Using organic materials as precursors for LDH modification is considered more environmentally friendly and has been shown to enhance the performance of LDH as an adsorbent. For example, the addition of *Eucheuma cottonii*, a natural material, has successfully improved LDH's structural stability, allowing it to be reused for anionic dye adsorption across 4-5 cycles [20]. Similarly, LDH modified with spirulina has demonstrated increased adsorption capacity for malachite green dye, with over 90% efficiency maintained across four cycles [21]. These findings highlight the potential of natural materials as effective LDH supports, with *Uncaria gambir* being a particularly promising candidate.

Uncaria gambir is one of the organic materials that can be used to composite with LDH because bioactive compounds, especially catechins, account for more than 90% mg CE [22]. Catechins are polyphenolic compounds with abundant hydroxyl (-OH) groups, making them highly reactive towards various types of pollutants [23]. These -OH groups play an essential role in increasing adsorption capacity as they can interact with pollutant molecules through hydrogen bonding and electrostatic interactions [24]. In the context of compositing with materials such as LDH, the functional groups of catechins not only help increase the adsorption capacity but also stabilize the material's structure, making it more durable and effective in the adsorption and regeneration process.

In this study, the adsorption ability of NiFe LDH was enhanced by addition of the organic material such as gambier leaf using the co-precipitation method. The resulting composites were identified using XRD, FTIR, and BET techniques. Adsorption experiments were performed on both NiFe LDH and NiFe-UG LDH using malachite green dye, with variables including pH value, contact period, dye concentration, and temperature. Additionally, the structural stability of the materials was evaluated through regeneration tests involving multiple cycles of use.

2. Materials and Methods

2.1 Chemical and Instrumentation

The substances used in this research included Gambier leaf (*Uncaria gambir*) sourced from the village of Babat Toman, Indonesia, malachite green, ethyl acetate ($CH_3COOCH_2CH_3$), sodium carbonate (Na_2CO_3), sodium hydroxide (NaOH), nickel(II) nitrate ($Ni(NO_3)_2.6H_2O$), iron(III) nitrate ($Fe(NO_3)_3.9H_2O$, and hydrochloride acid (HCl) which was purchased from Merck without purification.

In addition, the equipment used included analytical balance, standard glassware, orbital shaker, oven, pH meter, BELSORP-miniX Brunauer–Emmett–Teller (BET) surface area analyzer, Rigaku Miniflex XRD, Shimadzu Prestige-21 Fourier Transform Infrared spectrophotometer and Biobase BK-UV 1800 PC series UV-Vis Spectrophotometer.

2.2 Extraction of Gambier Leaves (*Uncaria gambir*)

The extraction process of gambier leaves was conducted following the method outlined by Pramanik *et al*. [25]. Fresh gambier leaves were dried under sunlight to reduce moisture content and then pulverized into a fine powder to increase the surface area for optimal extraction. In total, 300 mg of the powdered leaves was soaked in 500 mL of ethyl acetate for 72 hours, with the solution refreshed every 24 hours to maximize the extraction of bioactive compounds. After filtration, the resulting liquid extract was concentrated using a rotary evaporator at 50 °C, followed by drying and grinding to achieve a fine consistency. To ensure reliability, this extraction procedure was repeated three times. The yield of the extracted gambier leaves was calculated using the Equation (1):

$$\%Yield = \frac{Weight\ of\ Extract\ Obtained}{Initial\ Weight\ of\ Gambier\ Leaves\ Used} x100\% \quad (1)$$

2.3 Synthesize of NiFe LDH

Synthesis of NiFe LDH using the co-precipitation technique. Nickel(II) nitrate and iron(III) nitrate were mixed in a concentration ratio of (0.75 M : 0.25 M). Then 2 M NaOH and 2 M Na_2CO_3 were added to alkaline conditions (pH = 8). The mixture was continuously stirred and

Copyright © 2024, ISSN 1978-2993

heated to 80 °C for a duration of 17 hours. The settled sludge was filtered, dried, and pulverized to powder form.

2.4. Synthesize of NiFe-UG LDH

The composite of NiFe-UG LDH was conducted using an aqueous solution. 3 g of NiFe LDH was combined with 50 mL of aquadest and subjected to sonication for 30 minutes. Subsequently, 3 g of gambier extract was added and mixed for 24 hours at 80 °C. This procedure was carried out in a nitrogen-enriched environment.

2.5. Adsorption Experiment

2.5.1 Determinant of pH_{pzc} and pH impact

The determination of the pH point of zero charge (pH_{pzc}) of adsorbent materials is used to understand the interaction between adsorbents and ions in solution. A total of 20 mL of 2 M NaCl solution was used as a neutral solution, which was then varied in pH from 3 to 11. The adsorbent material was then added up to 20 mg and stirred for 24 hours, after which the final pH was measured. Each pH measurement was conducted in triplicate to ensure repeatability and consistency of results. The pH_{pzc} was obtained from a plot of the initial pH and the ΔpH as follows in Equation 2.

$$\Delta pH = pH_{final} - pH_{initial} \quad (2)$$

To determine the pH optimum for each adsorbent, adsorption experiments were conducted over the same pH ranges of 3-11. The adsorption capacity was measured at each pH level to identify the pH at which the adsorbent exhibited maximum adsorption efficiency. The optimum pH was determined by comparing the dye adsorbed ($C_{initial} - C_{final}$) at various pH values. This pH was then compared to the pH_{pzc} to evaluate the influence of the surface charge of the adsorbent on the adsorption process.

2.5.2 Contact time impact

Contact time was studied to determine the optimum time and kinetics of adsorption. contact time variations were carried out with a time range of 0-120 minutes in the optimum pH atmosphere on each adsorbent. Each contact time measurement was conducted in triplicate to ensure repeatability and consistency of results. The optimum time was observed when the adsorption capacity was in a state of equilibrium. The adsorption kinetics were analyzed using pseudo-first-order (PFO) and pseudo-second-order (PSO). The PFO is shown in Equation (3).

$$log\ (Q_e - Q_t) = log\ Q_e - \frac{k_1}{2.303t} \quad (3)$$

where Q_e is the amount of dye adsorbed at equilibrium (mg/g), Q_t is the amount adsorbed at time t (mg/g), k_1 is the rate constant of the PFO adsorption (1/min), and t is time (min). The rate constant k_1 can be determined from the slope of the linear plot of log (Q_e-Q_t) versus t. Then, PSO is given in Equation (4).

$$\frac{t}{Q_t} = \frac{1}{k_2 Q_e^2} + \frac{1}{Q_e} \quad (4)$$

where, k_2 is the PSO rate constant (g/mg.min), and the rate constant k_2 can be determined from the plot of t/Q_t versus t.

2.5.4 Concentration and temperature impact

Concentration and temperature experiments are used to study isotherms and thermodynamics study. The MG concentration was varied at 60, 80, 100, and 120 mg/L, while the temperature ranged from 40 °C to 60 °C. Each concentration and temperature measurement was conducted in triplicate to ensure repeatability and consistency of results. At pH and contact time optimum, equilibrium studies were carried out by fitting the experimental data to Langmuir and Freundlich isotherm. The Langmuir isotherm is represented by Equation (5).

$$\frac{1}{Q_e} = \frac{1}{Q_{max}} + \frac{1}{K_L Q_{max} C_e} \quad (5)$$

It was used to calculate the maximum adsorption capacity (Q_{max}) and the Langmuir constant (K_L), indicating the affinity of adsorption MG. The Freundlich isotherm is given in Equation (6).

$$\log Q_e = \log K_F + \frac{1}{n} \log C_e \quad (6)$$

It was used to describe adsorption on heterogeneous surfaces, where K_F and n were obtained to evaluate adsorption capacity and intensity, respectively.

To investigate the nature of the adsorption process, thermodynamic parameters were calculated by conducting adsorption experiments at different temperatures. The Gibbs free energy change (ΔG°) was determined using the Equation (7).

$$\Delta G^o = -RT \ln K_d \quad (7)$$

where, K_d is the distribution coefficient, R is the gas constant, and T is the temperature in Kelvin. The enthalpy change (ΔH°) and entropy change (ΔS°) were calculated from Equation (8).

Copyright © 2024, ISSN 1978-2993

$$\ln K_d = \frac{\Delta S^o}{R} - \frac{\Delta H^o}{RT} \quad (8)$$

The plot ln K_d versus $\frac{1}{T}$ was used to derive the values of $\Delta H°$ and $\Delta S°$.

2.5.5 Regeneration of adsorbent

The stability of the adsorbent was investigated through MG adsorption over 5 cycles. NiFe and NiFe-UG LDH were used to adsorb MG under optimum pH and contact time conditions. After each adsorption process, the adsorbent was separated from the adsorbate, then ultrasonicated and dried before reuse. For reliability, each cycle was conducted in triplicate, and adsorption efficiency (%E) was measured for each cycle according to Equation (9).

$$\%E = \frac{C_{initial} - C_{final}}{C_{initial}} x100\% \quad (9)$$

3. Results and Discussion

3.1 Characterization of Adsorbent

The diffractogram of Gambier extract displays peaks at 16.83° and 21.81° (Figure 1(a)), indicating the presence of secondary metabolites such as catechins and anhydrous catechin (tannins) [26]. The NiFe LDH diffractogram shows characteristic peaks at 11.48° (003), 22.96° (006), 34.47° (012), 38.56° (015), 45.89° (018), and 61.31° (110), which are consistent with the JCPDS standard (40-0215) [27,28]. These peaks confirm the successful synthesis of the LDH structure. Upon modification with Gambier extract, a new peak appears at 18.43°, pointing to the incorporation of Gambier's bioactive compounds into the LDH matrix. The slight shift of the d_{006} peak from 22.96° to 23.02° further suggests an interaction between the LDH surface and the Gambier metabolites, confirming the formation of the NiFe-Gambier composite and showing that structural changes have occurred due to the Gambier addition.

Fourier-transform infrared (FT-IR) analysis provides further insight into the structural integration between NiFe LDH, Gambier extract, and the NiFe-UG composite (Figure 1(b)). The NiFe LDH spectrum shows bands at 3456 cm^{-1} and 1643 cm^{-1}, which correspond to O–H stretching and H–O–H bending vibrations, respectively, indicating water molecules in the interlayer structure and on the surface of LDH [29]. The peak at 1367 cm^{-1} is attributed to interlayer anions ($–NO_3^-$) [30], while bands at 760

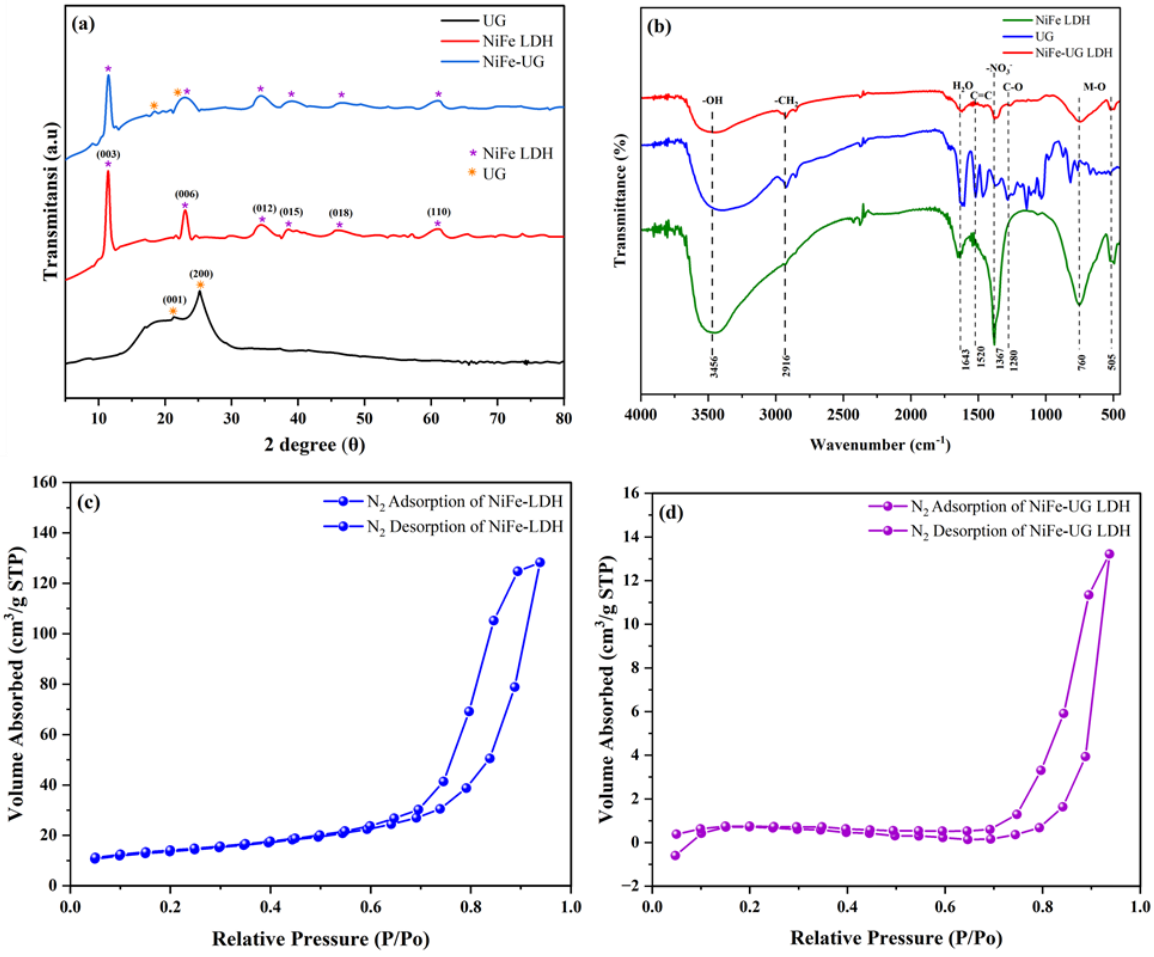

Figure 1. XRD difractogram (a), spectra of FTIR (b), and N_2 adsorption-desorption (c and d) of NiFe LDH and NiFe-UG LDH

Copyright © 2024, ISSN 1978-2993

cm^{-1} and 505 cm^{-1} correspond to Ni–O or Fe–O bonds, characteristic of the LDH's metal-oxygen framework [31]. In the NiFe-UG spectrum, new peaks appear at 1520 cm^{-1} and 1280 cm^{-1}, associated with C=C and C–O bonds, confirming the interaction of Gambier extract with the LDH through the presence of secondary metabolites [32]. This FT-IR evidence supports the XRD results, showing that Gambier extract not only binds to the LDH surface but also causes structural changes.

BET analysis and nitrogen adsorption-desorption isotherms (Figures 1(c) and 1(d)) reveal nearly uniform isotherm characteristics for both NiFe LDH and NiFe-UG LDH. Both materials exhibit a type IV isotherm with a hysteresis loop, typical of mesoporous materials, signifying a uniform pore size distribution. Despite the similar isotherm shape, significant differences in surface area and pore size are observed, supporting the findings of XRD and FT-IR, which indicate that structural changes due to Gambier extract affect the material's porosity and surface area, ultimately impacting adsorption performance.

According to the BET analysis data in Table 1, NiFe LDH features a surface area of 47.087 m^2/g, an average pore size of 8.450 nm, and a total pore volume of 0.198 cm^3/g. With these attributes, it can be classified as mesoporous (2-50 nm) [33], a structure that is well-suited to adsorb larger molecules like Malachite Green (MG), thanks to its numerous active sites and defined pathways for diffusion. Upon modification with Gambier extract, however, the surface area of NiFe-UG LDH drops significantly to 1.554 m^2/g, with a total pore volume reduced to 0.020 cm^3/g, despite an increased average pore size of 26.373 nm. This increase in pore size could support the diffusion of larger molecules, yet the substantial reduction in surface area limits the overall adsorption potential and reduces the number of accessible active sites [34].

Table 1. BET data of NiFe LDH and NiFe-UG LDH

Material	Surface Area (m^2/g)	Average Pore Size (nm)	Total Pore Volume (cm^3/g)
NiFe LDH	47.087	8.450	0.198
NiFe-UG LDH	1.554	26.373	0.020

The BET findings confirm structural interactions noted in both XRD and FT-IR analyses. Gambier extract appears to block smaller pores or aggregate particles within the LDH (illustrated in Figure 2), leading to a decrease in active surface sites [35]. Although the larger pores in NiFe-UG LDH may facilitate access for sizable molecules, the restricted surface area results in a lower adsorption efficiency than that of NiFe LDH.

3.2. Adsorption Performance

3.2.1 pH impact

pH is essential for the adsorption process which can affect the charge on the adsorbent surface and the ionization state of the adsorbate [36,37]. To determine the stability of the charge on the material surface can be determined by measuring the pH_{pzc} [38,39]. In the case of NiFe LDH and NiFe-UG LDH, the pH_{pzc} values are 6.913 and 7.105, respectively (Figure 3). This suggests that at pH levels greater than pHpzc, the surface becomes negatively charged, increasing its ability to absorb cationic dyes such as MG. In contrast, when the pH is below the pH_{pzc}, the surface has a positive charge [40,41]. For malachite green adsorption, the optimal pH values are 9 for NiFe LDH and 8 for NiFe-UG LDH, which are both higher than their respective pH_{pzc} values. This suggests that MG dye adsorption is mediated by electrostatic interactions between the adsorbent surface and ions in the solution.

3.2.2 Contact time impact

To determine the optimal time required for the adsorbent to adsorb Malachite Green (MG),

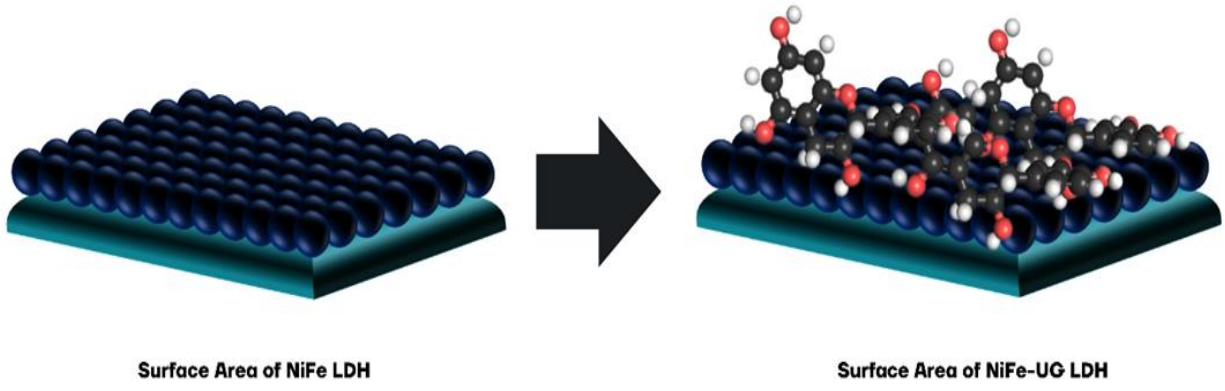

Figure 2. Illustration of reduced surface area

Copyright © 2024, ISSN 1978-2993

the effect of contact time was studied. Figure 4 illustrates that as time increases, the adsorption of MG by both NiFe LDH and NiFe-UG LDH also increases. Specifically, NiFe-UG LDH achieves its optimal adsorption capacity at a contact time of 70 minutes, which is faster than NiFe LDH, which requires 100 minutes to reach the same state. This quicker adsorption rate in NiFe-UG may be influenced by additional functional groups introduced by gambier extract. These groups likely enhance MG diffusion into NiFe-UG's surface, thereby increasing adsorption efficiency within a shorter time frame.

The adsorption kinetics for both NiFe LDH and NiFe-UG LDH are depicted in Figure 4, which reveals significant insights into the adsorption rate between the adsorbent and the adsorbate. Adsorption kinetics analysis provides crucial information on how quickly adsorption equilibrium can be achieved, a key factor in practical applications [42]. In this study, both adsorbents adhered to a pseudo-first-order (PFO) kinetic model. This is supported by the correlation coefficient values (R^2) shown in Table 2, where R^2 for the PFO model is higher than for the pseudo-second-order (PSO) model.

Additionally, the adsorption capacities in the PFO model-experimental ($Q_{e\ exp}$) and calculated ($Q_{e\ calc}$) are closely matched, further confirming that the adsorption process of MG on NiFe-based adsorbents is driven by surface-active sites. These findings underscore the importance of active sites on the adsorbent surface in facilitating rapid and effective adsorption of MG.

3.2.3 Concentration and temperature impact

The concentration variation in MG adsorption by NiFe LDH and NiFe-UG LDH was analyzed to understand the underlying adsorption mechanisms. Adsorption isotherms, specifically the Langmuir and Freundlich models, were applied to assess these mechanisms. As indicated in Table 3, NiFe-UG LDH aligns with the Langmuir isotherm model, suggesting monolayer

Table 2. Determination of PFO and PSO of NiFe LDH and NiFe-UG LDH

Adsorbent	Q_e Exp (mg/L)	PFO			PSO		
		$Q_{e\ Calc}$ (mg/L)	k_1	R^2	$Q_{e\ Calc}$ (mg/L)	k_2	R^2
NiFe LDH	35.980 ± 0.003	35.609 ± 0.383	0.057 ± 0.003	0.993	41.136 ± 0.961	0.002 ± 2.388E-4	0.987
NiFe-UG LDH	38.500 ± 0.012	38.520 ± 0.341	0.101 ± 0.006	0.992	41.472 ± 1.070	0.004 ± 0.001	0.972

Table 3. Isotherm adsorption of NiFe LDH and NiFe-UG LDH

Material	T (°C)	Langmuir			Freundlich		
		Q_{max}	K_L	R^2	n	K_F	R^2
NiFe LDH	60	58.487 ± 30.037	0.124 ± 0.075	0.6262	0.433 ± 0.127	2.642 ± 3.139	0.847
NiFe-UG	60	41.927 ± 6.570	3.652 ± 1.617	0.9627	1.449 ± 0.23	0.5644 ± 0.0097	0.951

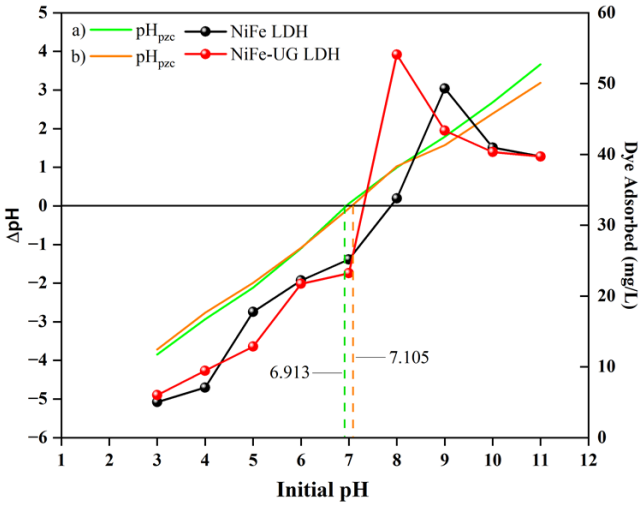

Figure 3. Optimum pH and pH_{pzc} of NiFe LDH and NiFe-UG

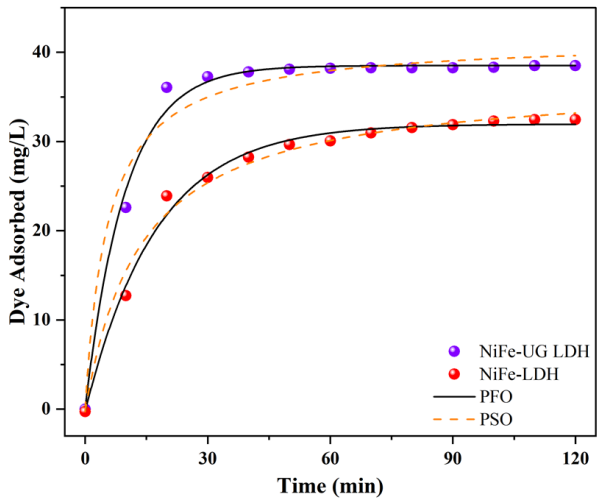

Figure 4. Contact time and adsorption kinetic of NiFe LDH and NiFe-UG LDH

Copyright © 2024, ISSN 1978-2993

adsorption on a homogeneous surface with specific interactions between adsorbent and adsorbate [43]. This is notable because, despite its smaller surface area, NiFe-UG LDH effectively utilizes active sites due to the uniform surface properties and the presence of functional groups from the gambier extract. These functional groups, like -OH and catechins, enhance bonding affinity with MG through hydrogen bonding or electrostatic interactions, making the adsorption process more efficient.

In contrast, NiFe LDH follows the Freundlich isotherm model, typically associated with adsorption on heterogeneous surfaces with varying adsorption energies [44]. Despite NiFe LDH's larger surface area, its adsorption capacity is lower, as seen in Table 5, where NiFe LDH's maximum adsorption capacity (Q_{max}) of 58.487 ± 30.037 mg/g is higher than NiFe-UG LDH's 41.927 ± 6.570 mg/g, yet both still fall within competitive ranges relative to other adsorbents, such as MgCr LDH and ZnAl-[$SiW_{12}O_{40}$] [45,46]. The less efficient contact in NiFe LDH results from its heterogeneous surface, reducing its effectiveness compared to the uniformly modified surface of NiFe-UG LDH.

The thermodynamic parameters for MG adsorption on both NiFe LDH and NiFe-UG LDH, shown in Table 4, provide additional insights into the adsorption process. For NiFe LDH, the negative Gibbs free energy (ΔG°) values confirm the spontaneity of the adsorption process, while the positive enthalpy change (ΔH°) indicates that the adsorption is endothermic, suggesting weak interactions between MG and the adsorbent surface [47]. The positive entropy change (ΔS°) observed further implies an increase in randomness at the solid-liquid interface, a typical feature of physisorption [48].

NiFe-UG LDH, which also exhibited negative ΔG° values, confirms spontaneity in the adsorption process. However, the comparatively higher ΔH° values for NiFe-UG LDH suggest stronger and more complex interactions between MG and the adsorbent, likely due to the additional hydroxyl and catechin groups from the gambier extract that enhance binding affinity [49]. This increase in binding complexity corresponds to the greater energy requirement for NiFe-UG LDH adsorption. Additionally, the positive ΔS° value aligns with the increased randomness at the interface, similar to the trend seen in NiFe LDH, further reinforcing the stability and efficiency of NiFe-UG in capturing MG molecules. The thermodynamic and isotherm data, together with the adsorption efficiency comparisons in the table, demonstrate that NiFe-UG LDH's performance is favorable not only due to its structural properties but also because of the beneficial modifications from the gambier extract.

3.2.4 Regeneration of adsorbent

The regeneration process enhances the adsorbent's cost-effectiveness and sustainability by enabling multiple reuses [50], reducing the overall operational costs associated with fresh adsorbent materialsdy evaluated the stability of NiFe LDH and NiFe-UG LDH adsorbents over five adsorption-desorption cycles, using ultrasonic assistance to improve the regeneration process. As illustrated in Figure 5, both adsorbents demonstrated commendable reusability, with NiFe-UG LDH showing a marginally higher adsorption efficiency compared to NiFe LDH.

Table 4. Thermodynamics adsorption of NiFe LDH and NiFe-UG LDH

Material	C (mg/L)	ΔH ° (kJ/mol)	ΔS° (kJ/mol)	ΔG° (kJ/mol			
				303 K	313 K	323 K	333 K
NiFe LDH	120	33.964 ± 2.168	0.125 ± 0.007	−3.911 ± 2.177	−5.161 ± 2.179	−6.411 ± 2.179	−7.661 ± 2.179
NiFe-UG	120	40.507 ± 4.928	0.154 ± 0.016	−6.155 ± 6.906	−7.655 ± 7.034	−9.155 ± 7.141	−10.655 ± 7.249

Table 5. Comparison of adsorption capacity of various materials on MG

Materials	Time (min)	Q_{max} (mg/g)	References
Rice Husk	60	6.500	[51]
ZnAl-[$SiW_{12}O_{40}$]	120	37.514	[46]
PMMA/GO-Fe_3O_4	35	3.500	[52]
Jack Fruit Ash	165	20.410	[53]
Catha edulis	60	5.620	[54]
Artemit	160	10.058	[55]
Clay-Biochar	120	12.125	[56]
MgCr LDH	70	33.784	[45]
NiFe LDH	100	58.487	This study
NiFe-UG	70	41.927	This study

Copyright © 2024, ISSN 1978-2993

Specifically, the adsorption efficiency for NiFe-UG LDH decreased from 96.420% in the first cycle to 86.614% in the fifth, while NiFe LDH showed a slight drop from 92.085% to 86.305%. This consistent performance indicates that the structural integrity and active adsorption sites of both materials are largely preserved across multiple cycles. However, the slightly superior performance of NiFe-UG LDH can be attributed to the functional groups provided by the gambier extract, which may enhance stability and reinforce the binding affinity with MG. These results underscore the practicality of NiFe-UG LDH as a sustainable adsorbent choice, with enhanced regeneration capacity that supports prolonged usage and reduces waste, thereby adding value to wastewater treatment applications.

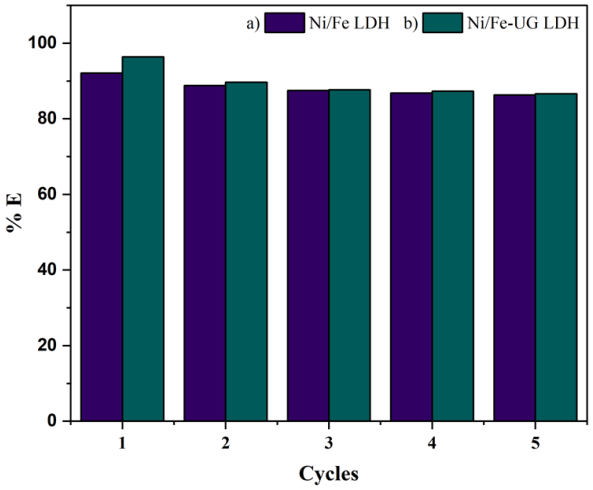

Figure 5. Regeneration of NiFe LDH and NiFe-UG LDH

3.2.5 Adsorption mechanism of MG

The adsorption mechanism envisioned in this study is illustrated in Figure 6. The optimum pH of both adsorbents is above the pH_{pzc}, indicating that the surface of the material is negatively charged. This may lead to electrostatic interactions in the MG adsorption process with both NiFe LDH and NiFe-UG. Based on the results of pH, contact time, concentration, and temperature tests, NiFe LDH adsorbs by physisorption mechanism. On the other hand, NiFe-UG adsorbs MG by a combination of physisorption-chemisorption mechanisms. This is indicated by the interaction of hydroxyl groups and catechins with adsorbate. This is also shown in the FT-IR Spectra before and after adsorption (Figure 7), where there was a change in intensity at wavenumbers 1643, 1367, and 760 cm^{-1}.

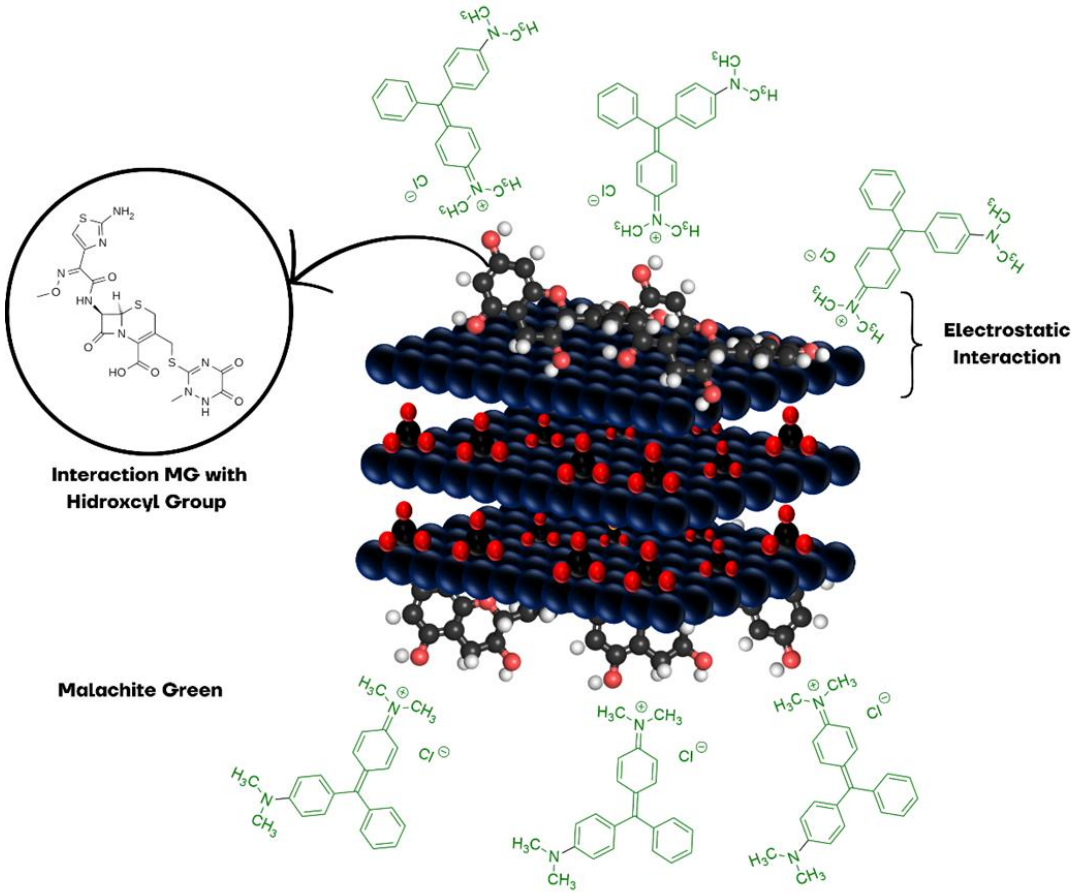

Figure 6. Mechanism of adsorption of Malachite Green

Copyright © 2024, ISSN 1978-2993

4. Conclusions

This study successfully synthesized NiFe LDH and NiFe-UG LDH for the treatment of Malachite Green (MG) dye, highlighting key factors such as pH, contact time, concentration, and temperature in the adsorption process. The optimal pH for MG adsorption was 9 for NiFe LDH and 8 for NiFe-UG LDH, enhancing electrostatic interactions due to the negatively charged surfaces. NiFe-UG LDH exhibited a faster adsorption capacity, reaching its peak in 70 minutes, compared to 100 minutes for NiFe LDH, likely due to functional groups from gambier extract that facilitate MG diffusion. Experimental results showed NiFe-UG LDH had a higher adsorption efficiency of 96.420% versus 92.085% for NiFe LDH, with both following a pseudo-first-order kinetic model. Adsorption isotherm analysis indicated that NiFe-UG LDH adheres to the Langmuir model, suggesting monolayer adsorption, while NiFe LDH follows the Freundlich model, indicating a heterogeneous surface. Thermodynamic studies confirmed that both reactions were spontaneous and endothermic, with NiFe-UG requiring more energy. High stability was observed in reusability tests for both materials, underscoring their practical applicability in wastewater treatment. The study concludes that the adsorption mechanism in NiFe primarily operates through physisorption, whereas NiFe-UG involves a combination of physisorption and chemisorption. Future research should focus on modifications to enhance adsorption efficiency and evaluate effectiveness against a wider range of pollutants.

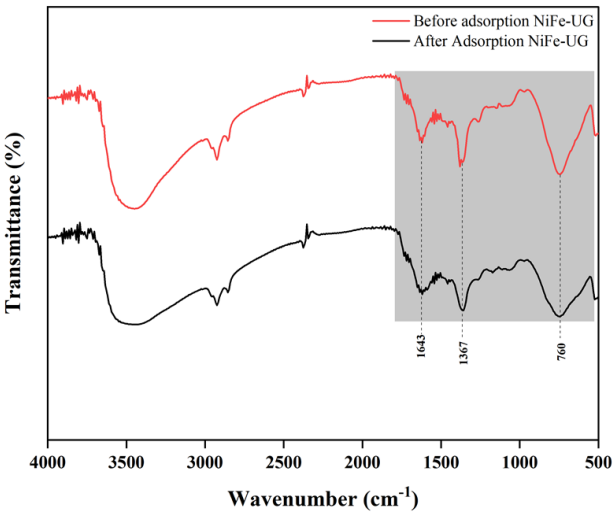

Figure 7. FTIR spectra of before-after adsorption of Malachite Green dye

Acknowledgment

Appreciation and gratitude to the Research Center of Inorganic Materials and Complexes, Faculty of Mathematics and Natural Sciences,, Sriwijaya University, for helping in discussions and assisting in this study.

CRediT Author Statement

Jefri Jefri: Conceptualization, Investigation, Writing – Original draft, Software. Najma Annuria Fithri: Methodology, Validation, Visualization, Conceptualization. Aldes Lesbani: Methodology, Conceptualization, Writing – review & editing, Supervision. All authors have read and agreed to the published version of the manuscript.

References

[1] Ayuz Firstian Adjid, G., Kurniawan, A. (2022). Textile Industry Waste Pollution in the Konto River: A Comparison of Public Perceptions and Water Quality Data. *The Journal of Experimental Life Science*, 12 (3), 105–113. DOI: 10.21776/ub.jels.2022.012.03.05

[2] Ahmad Khan, F., Dar, B.A., Farooqui, M. (2023). Characterization and Adsorption of Malachite Green Dye from Aqueous Solution onto *Salix alba* L. (Willow Tree) Leaves Powder and Its Respective Biochar. *International Journal of Phytoremediation*, 25(5), 646–657. DOI: 10.1080/15226514.2022.2098909.

[3] Abewaa, M., Mengistu, A., Takele, T., Fito, J., Nkambule, T. (2023). Adsorptive Removal of Malachite Green Dye from Aqueous Solution Using *Rumex abyssinicus* Derived Activated Carbon. *Scientific Reports*, 13(1). DOI: 10.1038/s41598-023-41957-x.

[4] Palapa, N.R., Amri, A., Hanifah, Y. (2023). Potential Indonesian Rice Husk for Wastewater Treatment Agricultural Waste Preparation and Dye Removal Application. *Indonesian Journal of Environmental Management and Sustainability*, 7 (4), 160–165. DOI: 10.26554/ijems.2023.7.4.160-165.

[5] De Almada Vilhena, A.O., Lima, K.M.M., De Azevedo, L.F.C., Rissino, J.D., De Souza, A.C.P., Nagamachi, C.Y., Pieczarka, J.C. (2023). The Synthetic Dye Malachite Green Found in Food Induces Cytotoxicity and Genotoxicity in Four Different Mammalian Cell Lines from Distinct Tissuesw. *Toxicology Research*, 12(4), 693–701. DOI: 10.1093/toxres/tfad059.

[6] Sharma, J., Sharma, S., Soni, V. (2023). Toxicity of Malachite Green on Plants and Its Phytoremediation: A Review. *Regional Studies in Marine Science*, 62, 102911. DOI: 10.1016/J.RSMA.2023.102911.

[7] Sadegh, N., Haddadi, H., Sadegh, F., Asfaram, A. (2023). Recent Advances and Perspectives of Tannin-Based Adsorbents for Wastewater Pollutants Elimination: A Review. *Environmental Nanotechnology, Monitoring & Management*, 19, 100763. DOI: 10.1016/j.enmm.2022.100763.

Copyright © 2024, ISSN 1978-2993

[8] Pathy, A., Krishnamoorthy, N., Chang, S.X., Paramasivan, B. (2022). Malachite Green Removal Using Algal Biochar and Its Composites with Kombucha SCOBY: An Integrated Biosorption and Phycoremediation Approach. *Surfaces and Interfaces*, 30, 101880. DOI: 10.1016/j.surfin.2022.101880.

[9] Hussien Hamad, M.T.M. (2023). Optimization Study of the Adsorption of Malachite Green Removal by MgO Nano-Composite, Nano-Bentonite and Fungal Immobilization on Active Carbon Using Response Surface Methodology and Kinetic Study. *Environmental Sciences Europe*, 35(1). DOI: 10.1186/s12302-023-00728-1.

[10] Abbas, M., Trari, M. (2023). Contribution of Zeolite to Remove Malachite Green in Aqueous Solution by Adsorption Processes: Kinetics, Isotherms and Thermodynamic Studies. *Textile Research Journal*, 93(15–16), 3765–3776. DOI: 10.1177/00405175231165336.

[11] Yuliasari, N., Wijaya, A., Mohadi, R., Elfita, E., Lesbani, A. (2022). Photocatalytic Degradation of Malachite Green by Layered Double Hydroxide Based Composites. *Bulletin of Chemical Reaction Engineering and Catalysis*, 17 (2), 240–249. DOI: 10.9767/bcrec.17.2.13482.240-249.

[12] Mohapi, M., Sefadi, J.S., Mochane, M.J., Magagula, S.I., Lebelo, K. (2020). Effect of LDHs and Other Clays on Polymer Composite in Adsorptive Removal of Contaminants: A Review. *Crystals*, 10(11). DOI: 10.3390/cryst10110957.

[13] Farhan, A., Khalid, A., Maqsood, N., Iftekhar, S., Sharif, H.M.A., Qi, F., Sillanpää, M., Asif, M.B. (2024). Progress in Layered Double Hydroxides (LDHs): Synthesis and Application in Adsorption, Catalysis and Photoreduction. *Science of The Total Environment*, 912, 169160. DOI: 10.1016/j.scitotenv.2023.169160.

[14] Hanifah, Y., Amri, A. (2023). Preparation of Layered Double Hydroxide-Polyoxometalate Based Composite. *Indonesian Journal of Material Research*, 1(2), 68–73. DOI: 10.26554/ijmr.20231210.

[15] Wang, Y., Yan, D., El Hankari, S., Zou, Y., Wang, S. (2018). Recent Progress on Layered Double Hydroxides and Their Derivatives for Electrocatalytic Water Splitting. *Advanced Science*, 5 (8), 1800064. DOI: https://doi.org/10.1002/advs.201800064.

[16] Palapa, N.R., Saria, Y., Taher, T., Mohadi, R., Lesbani, A. (2019). Synthesis and Characterization of Zn/Al, Zn/Fe, and Zn/Cr Layered Double Hydroxides: Effect of M^{3+} Ions Toward Layer Formation. *Science and Technology Indonesia*, 4 (2), 36–39. DOI: 10.26554/sti.2019.4.2.36-39.

[17] Mittal, J. (2021). Recent Progress in the Synthesis of Layered Double Hydroxides and Their Application for the Adsorptive Removal of Dyes: A Review. *Journal of Environmental Management*, 295, 113017. DOI: 10.1016/j.jenvman.2021.113017.

[18] Nava-Andrade, K., Carbajal-Arízaga, G.G., Obregón, S., Rodríguez-González, V. (2021). Layered Double Hydroxides and Related Hybrid Materials for Removal of Pharmaceutical Pollutants from Water. *Journal of Environmental Management*, 288, 112399. DOI: 10.1016/j.jenvman.2021.112399.

[19] Ahmad, N., Suryani Arsyad, F., Royani, I., Mega Syah Bahar Nur Siregar, P., Taher, T., Lesbani, A. (2023). High Regeneration of ZnAl/NiAl-Magnetite Humic Acid for Adsorption of Congo Red from Aqueous Solution. *Inorganic Chemistry Communications*, 150, 110517. DOI: 10.1016/j.inoche.2023.110517.

[20] Wibiyan, S., Royani, I., Ahmad, N., Lesbani, A. (2024). Assessing the Efficiency, Selectivity, and Reusability of ZnAl-Layered Double Hydroxide and *Eucheuma cottonii* Composite in Removing Anionic dyes from wastewater. *Inorganic Chemistry Communications*, 170, 113347. DOI: 10.1016/j.inoche.2024.113347.

[21] Lesbani, A., Ahmad, N., Mohadi, R., Royani, I., Wibiyan, S., Amri, Hanifah, Y. (2024). Selective Adsorption of Cationic Dyes by Layered Double Hydroxide with Assist Algae (*Spirulina platensis*) to Enrich Functional Groups. *JCIS Open*, 15, 100118. DOI: 10.1016/j.jciso.2024.100118.

[22] Malrianti, Y., Kasim, A., Asben, A., Syafri, E., Yeni, G., Fudholi, A. (2021). Catechin Extracted from *Uncaria gambier* Roxb for Nanocatechin Production: Physical and Chemical Properties. *International Journal of Design and Nature and Ecodynamics*, 16 (4), 393–399. DOI: 10.18280/ijdne.160406.

[23] Cai, Z.-Y., Li, X.-M., Liang, J.-P., Xiang, L.-P., Wang, K.-R., Shi, Y.-L., Yang, R., Shi, M., Ye, J.-H., Lu, J.-L., Zheng, X.-Q., Liang, Y.-R. (2018). Bioavailability of Tea Catechins and Its Improvement. *Molecules*, 23 (9) DOI: 10.3390/molecules23092346.

[24] Li, H.Z., Zhang, Y.N., Guo, J.Z., Lv, J.Q., Huan, W.W., Li, B. (2021). Preparation of Hydrochar with High Adsorption Performance for Methylene Blue by Co-Hydrothermal Carbonization of Polyvinyl Chloride and Bamboo. *Bioresource Technology*, 337, 125442. DOI: 10.1016/j.biortech.2021.125442.

[25] Pramanik, F., Satari, M.H., Azhari, A. (2023). Cytotoxic Activity of Gambier Leave (*Uncaria gambir*) Ethyl Acetate Extract on Mouse Embryonic Fibroblast Cell (NIH-3T3) using MTT Assay. *The Open Dentistry Journal*, 17(1). DOI: 10.2174/18742106-v17-e230109-2022-78.

[26] Failisnur, F., Sofyan, S., Kasim, A., Angraini, T. (2018). Study of Cotton Fabric Dyeing Process with Some Mordant Methods by Using Gambier (*Uncaria gambir* Roxb) Extract. *International Journal on Advanced Science, Engineering and Information Technology*, 8(4), 1098–1104. DOI: 10.18517/ijaseit.8.4.4861.

Copyright © 2024, ISSN 1978-2993

[27] Wu, L., Yu, L., Zhang, F., Wang, D., Luo, D., Song, S., Yuan, C., Karim, A., Chen, S., Ren, Z. (2020). Facile Synthesis of Nanoparticle-Stacked Tungsten-Doped Nickel Iron Layered Double Hydroxide Nanosheets for Boosting Oxygen Evolution Reaction. *Journal of Materials Chemistry A*, 8(16), 8096–8103. DOI: 10.1039/D0TA00691B.

[28] Qian, J., Zhang, Y., Chen, Z., Du, Y., Ni, B.J. (2023). NiCo Layered Double Hydroxides/NiFe Layered Double Hydroxides Composite (NiCo-LDH/NiFe-LDH) Towards Efficient Oxygen Evolution in Different Water Matrices. *Chemosphere*, 345, 140472. DOI: 10.1016/j.chemosphere.2023.140472.

[29] Lesbani, A., Paruship, V., Rizki, M.F., Taher, T., Palapa, N.R., Mohadi, R. (2019). Preparation of M^{2+}/M^{3+} Layered Double Hydroxides (M^{2+}=Zn, Ni, M^{3+}=Fe): Effect of Different M^{2+} to the Layer Formation. In: *AIP Conference Proceedings*. American Institute of Physics Inc., p. 020055. DOI: 10.1063/1.5139787.

[30] Liu, X., Shi, J., Bai, X., Wu, W. (2021). Ultrasound-Excited Hydrogen Radical from NiFe Layered Double Hydroxide for Preparation of Ultrafine Supported Ru Nanocatalysts in Hydrogen Storage of N-Ethylcarbazole. *Ultrasonics Sonochemistry*, 81, 105840. DOI: 10.1016/j.ultsonch.2021.105840.

[31] Munonde, T.S., Zheng, H. (2021). The Impact of Ultrasonic Parameters on the Exfoliation of NiFe LDH Nanosheets as Electrocatalysts for the Oxygen Evolution Reaction in Alkaline Media. *Ultrasonics Sonochemistry*, 76, 105664. DOI: 10.1016/j.ultsonch.2021.105664.

[32] Shiyan, S., Safitri, I.N., Nathasia, J., Fitrotunnisa, L., Fransiska, O.L., Salsabillah, T., Pratiwi, G. (2023). FTIR Spectroscopy Combined with Chemometrics for Evaluation of Gambir Extract – Self Nano Emulsifying Formulation from *Uncaria gambir* Roxb. *Biointerface Research in Applied Chemistry*, 13(2), 1–11. DOI: 10.33263/briac132.153.

[33] Taylor, J.H., Masoudi Soltani, S. (2023). Carbonaceous Adsorbents in the Removal of Aquaculture Pollutants: A Technical Review of Methods and Mechanisms. *Ecotoxicology and Environmental Safety*, 266, 115552. DOI: 10.1016/j.ecoenv.2023.115552.

[34] Mane, P. V, Rego, R.M., Yap, P.L., Losic, D., Kurkuri, M.D. (2024). Unveiling Cutting-Edge Advances in High Surface Area Porous Materials for the Efficient Removal of Toxic Metal Ions from Water. *Progress in Materials Science*, 146, 101314. DOI: 10.1016/j.pmatsci.2024.101314.

[35] Ashraf, M.A., Peng, W., Zare, Y., Rhee, K.Y. (2018). Effects of Size and Aggregation/Agglomeration of Nanoparticles on the Interfacial/Interphase Properties and Tensile Strength of Polymer Nanocomposites. *Nanoscale Research Letters*, 13, 214. DOI: 10.1186/s11671-018-2624-0.

[36] Arab, C., El Kurdi, R., Patra, D. (2022). Effect of pH on the Removal of Anionic and Cationic Dyes Using Zinc Curcumin Oxide Nanoparticles as Adsorbent. *Materials Chemistry and Physics*, 277, 125504. DOI: 10.1016/j.matchemphys.2021.125504.

[37] Ahmad, N., Rohmatullaili, Wijaya, A., Lesbani, A. (2024). Magnetite Humic Acid-Decorated MgAl Layered Double Hydroxide and its Application in Procion Red Adsorption. *Colloids and Surfaces A: Physicochemical and Engineering Aspects*, 684 DOI: 10.1016/j.colsurfa.2023.133042.

[38] Wijaya, A., Zahara, A.Z., Siregar, P.M.S.B.N., Ahmad, N., Amri, A., Palapa, N.R., Lesbani, A. (2024). Cellulose-supported Ni/Al Layered Double Hydroxide (LDH) as Unique Adsorbents for Malachite Green Dye Removal in Aqueous Solutions. *Iranian of Journal Chemistry and Chemical Engineering*, 43 (4), 1566. DOI: 10.30492/ijcce.2024.1983141.5779.

[39] Amri, A., Lesbani, A., Mohadi, R. (2023). Malachite Green Dye Adsorption from Aqueous Solution using a Ni/Al Layered Double Hydroxide-Graphene Oxide Composite Material. *Science and Technology Indonesia*, 8(2), 280–287. DOI: 10.26554/sti.2023.8.2.280-287.

[40] Shkliarenko, Y., Halysh, V., Nesterenko, A. (2023). Adsorptive Performance of Walnut Shells Modified with Urea and Surfactant for Cationic Dye Removal. *Water (Switzerland)*, 15(8), 1536. DOI: 10.3390/w15081536.

[41] Saadi, A.S., Bousba, S., Riah, A., Belghit, M., Belkhalfa, B., Barour, H. (2024). Efficient Synthesis of Magnetic Activated Carbon from Oak Pericarp for Enhanced Dye Adsorption: A One-Step Approach. *Desalination and Water Treatment*, 319, 100420. DOI: 10.1016/j.dwt.2024.100420.

[42] Saleh, T.A. (2022). Kinetic Models and Thermodynamics of Adsorption Processes: Classification. *Interface Science and Technology*, 34, 65–97. DOI: 10.1016/B978-0-12-849876-7.00003-8.

[43] Brahma, D., Saikia, H. (2022). Synthesis of ZrO_2/MgAl-LDH Composites and Evaluation of Its Isotherm, Kinetics and Thermodynamic Properties in the Adsorption of Congo Red Dye. *Chemical Thermodynamics and Thermal Analysis*, 7, 100067. DOI: 10.1016/j.ctta.2022.100067.

[44] Chen, X., Ren, Y., Qu, G., Wang, Z., Yang, Y., Ning, P. (2023). A Review of Environmental Functional Materials for Cyanide Removal by Adsorption and Catalysis. *Inorganic Chemistry Communications*, 157, 111298. DOI: 10.1016/j.inoche.2023.111298.

[45] Badri, A.F., Mohadi, R., Mardiyanto, Lesbani, A. (2021). Adsorptive Capacity of Malachite Green onto Mg/M^{3+}(M3+=Al and Cr) Ldhs. *Global Nest Journal*, 23(1), 82–89. DOI: 10.30955/gnj.003443.

Copyright © 2024, ISSN 1978-2993

[46] Lesbani, A., Taher, T., Palapa, N.R., Mohadi, R., Mardiyanto, Miksusanti, Arsyad, F.S. (2021). Removal of Malachite Green Dye Using keggin Polyoxometalate Intercalated ZnAl Layered Double Hydroxide. *Walailak Journal of Science and Technology*, 18(10), 9414. DOI: 10.48048/wjst.2021.9414.

[47] Abewaa, M., Mengistu, A., Takele, T., Fito, J., Nkambule, T. (2023). Adsorptive Removal of Malachite Green dye from Aqueous Solution Using *Rumex abyssinicus* Derived Activated Carbon. *Scientific Reports*, 13(1), 14701. DOI: 10.1038/s41598-023-41957-x.

[48] Rosenholm, J.B. (2017). Critical Evaluation of Dipolar, Acid-Base and Charge interactions I. Electron Displacement within and Between Molecules, Liquids and Semiconductors. *Advances in Colloid and Interface Science*, 247, 264–304. DOI: 10.1016/j.cis.2017.06.004.

[49] Lu, H., Qi, Y., Zhao, Y., Jin, N. (2018). Effects of Hydroxyl Group on the Interaction of Carboxylated Flavonoid Derivatives with S. Cerevisiae α-Glucosidase. *Current Computer-Aided Drug Design*, 16(1), 31–44. DOI: 10.2174/1573409914666181022142553.

[50] Das, T., Debnath, A., Manna, M.S. (2024). Adsorption of Malachite Green by *Aegle marmelos*-Derived Activated Biochar: Novelty Assessment through Phytotoxicity Tests and Economic Analysis. *Journal of the Indian Chemical Society*, 101(9), 101219. DOI: 10.1016/j.jics.2024.101219.

[51] Muinde, V.M., Onyari, J.M., Wamalwa, B., Wabomba, J., Nthumbi, R.M. (2017). Adsorption of Malachite Green from Aqueous Solutions onto Rice Husks: Kinetic and Equilibrium Studies. *Journal of Environmental Protection*, 08(03), 215–230. DOI: 10.4236/jep.2017.83017.

[52] Rajabi, M., Mahanpoor, K., Moradi, O. (2019). Preparation of PMMA/GO and PMMA/GO-Fe_3O_4 Nanocomposites for Malachite Green Dye Adsorption: Kinetic and Thermodynamic Studies. *Composites Part B: Engineering*, 167, 544–555. DOI: 10.1016/j.compositesb.2019.03.030.

[53] Banerjee, S., Debsarkar, Dr.A., Datta, Dr.S. (2017). Adsorption of Methylene blue and Malachite Green in Aqueous Solution using Jack Fruit Leaf Ash as Low Cost Adsorbent. *International Journal of Environment, Agriculture and Biotechnology*, 2(3), 1396–1374. DOI: 10.22161/ijeab/2.3.45.

[54] Abate, G.Y., Alene, A.N., Habte, A.T., Getahun, D.M. (2020). Adsorptive Removal of Malachite Green Dye from Aqueous Solution onto Activated Carbon of *Catha edulis* Stem as a Low Cost Bio-Adsorbent. *Environmental Systems Research*, 9(1), 1. DOI: 10.1186/s40068-020-00191-4.

[55] Savci, S., Dönmez, S., Mazmanci, M.A. (2023). Performance and Mechanisms of Malachite Green Dye Adsorption Using Industrial Solid Waste as Adsorbent. *Environmental Engineering and Management Journal*, 22(1), 97–104. DOI: 10.30638/eemj.2023.009.

[56] Potgieter, J., Waanders, F.B., Fosso-Kankeu, E. (2019). Removal of Malachite Green and Toluidine Blue Dyes from Aqueous Solution Using a Clay-Biochar Composite of Bentonite and Sweet Sorghum bagasse. *International Journal of Applied Engineering Research*, 14(6), 1324–1333.

Copyright © 2024, ISSN 1978-2993